



Research Article

Fractional calculus modeling of cell viscoelasticity quantifies drug response and maturation more robustly than integer order models

Anh Vo¹ and Andrew Ekpenyong^{1,*}

¹ Department of Physics, Creighton University, 2500 California Plaza, Omaha, NE 68178, USA

* **Correspondence:** andrewekpenyong@creighton.edu; Tel: +1-402-280-2208; Fax: +1-402-280-2140.

Abstract: It has recently been discovered that the viscoelastic properties of cells are inherent markers reflecting the complex biological states, functions and malfunctions of the cells. Although the extraction of model parameters from the viscoelasticity data of many cell types has been done successfully using integer order mechanical and power-law viscoelastic models, there are some cell types and conditions where the goodness of fits falls behind. Thus, fractional order viscoelastic models have been proposed as more general and better suited for such modeling. In this work, we test such proposed generality using published data already fitted by integer order models. We find that cell viscoelasticity data can be fitted using fractional order viscoelastic models in more situations than integer order. For macrophages, which are among the white blood cells that function in the immune system, the fractional order Kelvin-Voigt model best captures pharmacological interventions and maturation of the cells. The steady state viscosity of macrophages decreases following depolymerization of F-actin using the drug cytochalasin D, and also decreases following myosin II breakdown using Blebbistatin. When macrophages are treated with a bacterium-derived chemoattractant, the steady state viscosity decreases. Interestingly, both the steady state viscosity and elastic modulus are progressively altered as the cells become mature and approach senescence. Taken together, these results show that fractional viscoelastic modeling, more robustly than integer order modeling, enables the further quantification of cell function and malfunction, with potential diagnostic and therapeutic applications especially in cases of cancer and immune system dysfunctions.

Keywords: cell mechanics, viscoelasticity, fractional calculus, fractional derivative, macrophages, cell compliance, cell deformability.

1. Introduction

The mechanical properties of cells such as viscosity and elasticity have emerged as critical parameters for understanding the cell's complex biological states, functions and malfunctions [1, 2, 3]. Viscosity is a measure of a fluid's resistance to flow when subjected to stress [4]. Elasticity is a measure of a body's ability to return to original dimensions following the application and removal of stress [5]. A viscoelastic material is therefore one that resists flow while also capable of partially returning to original dimensions after the removal of applied stress (for elaboration, see [5]). By resisting flow, viscoelastic materials dissipate mechanical energy. On the other hand, they partially return to original dimensions using stored mechanical energy. Thus, viscoelasticity is the exhibition of both viscous and elastic properties through simultaneous dissipation and storage of mechanical energy [6]. Biological cells are viscoelastic materials with a broad range of peculiar and adaptable features [7, 8, 1]. Measurements of mechanical properties of cells (and cellular constituents) such as their elasticity have been reported for decades [9, 10, 11]. But intensive research into cell mechanics, especially as an inherent marker of functional changes is a relatively recent and burgeoning enterprise. In response to mechanical loads or stress, biological cells usually deform in different ways. Cellular mechanics or cell rheology aims at quantifying these behaviors. Such quantitative understanding can help in clarifying biological phenomena, discovering new physics (of living matter) and providing clues for diagnostic and therapeutic applications in medicine. In this work, we use both integer order and non-integer order mechanical models to extract viscoelastic parameters from strain measurements carried out on special white blood cells. Our previous work using only integer order models [2] has been well received and confirmed by several other methods of measurements and analysis within broader cell physiology contexts [12, 13, 14, 15]. Hence, recent developments that show the utility of fractional viscoelastic models in systematically capturing material parameters for comparison across studies [16, 17] have directly given impetus to our extended analysis to include fractional viscoelastic models. It is pertinent to first describe stress, strain and the viscoelastic regimes we measured in order to set the stage for the modeling and characterization.

Considering stress and strain in general for a non-linear viscoelastic material, the stress, σ , can be expressed as $\sigma = F[\varepsilon(t), t]$ where ε is the time-dependent strain and F is a functional indicating both the properties of the material and the convolving conditions of measurement such as temperature and molecular perturbations. In the linear regime, the stress and time response can be separated so that we obtain a general expression for a linear viscoelastic material as $\sigma = \varepsilon G(t)$, where ε is the linear extensional strain and $G(t)$ is the time-dependent modulus of the material. Thus, in linear viscoelastic materials, the stress is proportional to the strain at all time points [18]. Many non-linear viscoelastic materials have a linear regime. In this regime, the mechanical properties of the material can be separated into an elastic recoverable part as Hooke's law (Eq. 1.1a) and the viscous part as Newton's law (Eq. 1.1b) [5],

$$\sigma = E\varepsilon \quad (1.1a)$$

$$\sigma = \eta \frac{d\varepsilon}{dt}. \quad (1.1b)$$

where E is Young's modulus (like spring stiffness) and η is the coefficient of viscosity (like dashpot viscosity). Obviously, such a separation is difficult in non-linear viscoelasticity. For the avoidance of confusion, we note that Eq. 1.1a applies to linear elasticity in one dimension. The 3D version is

$\sigma_{ij} = C_{ijkl}\varepsilon_{kl}$ [5]. An elastic but non-linear constitutive equation is given by

$$\sigma = f(\varepsilon)\varepsilon, \quad (1.2)$$

where $f(\varepsilon)$ is a non-linear function of strain. Both linear and non-linear elasticity have no time dependence. Thus, elastic materials recover fully and instantaneously when loaded or unloaded. Moreover, the path for loading is identical to the path of unloading, whether linear or non-linear.

For viscoelastic materials, a property that characterizes such materials when stress and strain functions are known is called the creep compliance, $J(t)$. In general, it is both time-dependent and stress-dependent and can therefore be denoted as $J(t, \sigma)$. Creep compliance with unit Pa^{-1} is usually measured through a creep-recovery test, where the stress is kept constant and the strain is recorded as a function of time (or conversely, through a strain-relaxation test, where the strain is kept constant and stress is recorded as a function of time). Mathematically, the constant stress in a creep recovery test can be expressed using the Heaviside step function $H(t)$, thus,

$$\sigma(t) = \sigma_0(H(t) - H(t - t_0)). \quad (1.3)$$

A material initially at rest at $t = t_0$, can be subjected to a constant stress σ_0 and the strain ε monitored as a function of time. Hence, the creep compliance can be defined as $J(t, \sigma_0) = \varepsilon(t)/\sigma$ so that using Eq. 1.3, we have,

$$J(t, \sigma) = \frac{\varepsilon(t)}{\sigma_0(H(t) - H(t - t_0))} \quad (1.4)$$

In the linear regime, which can be determined experimentally [19, 5], the stresses are small enough and the linear creep compliance $J(t)$ is obtained:

$$J(t, \sigma) \approx J(t). \quad (1.5)$$

Thus, using measured strain output and the known constant stress input, creep compliance for linear viscoelasticity is given by

$$J(t) = \frac{\varepsilon(t)}{\sigma_0}. \quad (1.6)$$

Creep compliance data for white blood cells are modeled in this work. The data were obtained by strain or deformation measurements using an optical stretcher, described in detail elsewhere [20, 21, 22, 2, 13, 14] and summarized in section 2 on materials and methods. We have used both ‘‘integer order’’ and fractional order derivatives to model our creep compliance data for cells. In modeling creep compliance data for tissues and tissue-like materials, it was shown that the fractional calculus (FC) models were better in fitting data [23], provoking the need to attempt this for cells. A recent review of the role of FC in modeling biological phenomena [24] shows increasing use of FC for more accurate modeling of diffusion of substances in the human body at the system and organ levels, and for viscoelasticity of tissues and action potentials in neurons. Attempts at standardization and generalization of viscoelastic characterization using FC, aimed at widespread adoption have emerged [16, 17]. Our work here shows that FC models accurately quantify the response of specific immune cells (here macrophages), to cytoskeletal drugs and chemical agents that signal bacterial infections, as well as their cellular maturation, just like the integer order models. Such quantification have implications for disease diagnosis and therapeutic options especially in the case of cancer, where alterations in cell mechanics not only indicate malignant transformation [20, 21, 25, 26] but have been identified as therapeutic target [27, 28].

2. Materials and methods

2.1. Measurement of viscoelastic properties of cells

In the optical stretcher, forces generated by the momentum transfer from two non-focused, counter-propagating, divergent laser beams to the surface of single suspended cells are employed to trap and deform the cells in a controlled and non-destructive way, thereby enabling the extraction of cell viscoelastic properties. Very instructive comparative reviews of most of the other methods of measuring cell mechanical properties can be found in [29, 30, 14]. There, micropipette aspiration, microplate manipulation, optical stretching and microfluidic deformation are evaluated together as techniques that measure global mechanical properties of cells. Furthermore, a different review [31] and designed experimental comparison [14] have been particularly useful in categorizing the techniques based on envisaged translation to clinical applications.

Let us focus on creep compliance as measured by the optical stretcher, OS. During a typical OS experiment, cells are introduced into a microfluidic delivery system, serially trapped and then stretched along the laser beam axis. The elongation of the cell body along the laser beam axis is recorded by a CCD camera. The time-dependent strain is extracted from the video camera images [2]. The axial strain during optical stretching is given by

$$\varepsilon = \frac{a(t)}{a_0} - 1, \quad (2.1)$$

where a_0 is the semi-major axis of the unstretched cell and $a(t)$ is the time-varying semi-major axis measured. The optically induced surface stress on the cells is computed using an electromagnetic wave model [32, 33], which requires knowledge of the average refractive index of cells. The average refractive index of cells was measured using a digital holographic microscope [34, 35]. Thus, the mechanical properties of cells obtained from OS measurements are decoupled from their optical characteristics. The tensile strain is normalized by the peak value of the calculated optical stress σ_0 and a geometric factor F_g to give the tensile compliance for each cell:

$$J(t) = \frac{\varepsilon(t)}{\sigma_0 F_g}. \quad (2.2)$$

Eq. 2.2 is identical to Eq. 1.6 except for the dimensionless F_g , which is calculated as described elsewhere [36] to account for cell shape and stress distribution. Insights into the often complex response of viscoelastic materials to stress or strain can be gained using appropriate assemblies of simple springs and dash pots which reflect the elastic and viscous aspects respectively. Also, scaling laws such as power law models can be used to analyze cellular viscoelastic responses [37, 3]. Relevant mechanical models are presented in the theory and calculation section. We next describe the intrinsic bases of the viscoelastic properties of cells, namely, cytoskeletal structures and how we altered these in order to obtain viscoelastic readouts.

2.2. Alterations of cytoskeletal structures and cell states

The typical eukaryotic cell has evolved structures in the cytoplasm and in the nucleus that enable it to perform the following mechanically relevant functions: spatial organization of its contents; physical

and biochemical connection to the external environment; and generation of coordinated forces that enable it to move and change shape [38]. These cytoskeletal structures, collectively called cytoskeleton, and the nuclear structures integrate the activity of a multitude of proteins and organelles. Let us focus on the cytoskeleton. The eukaryotic cytoskeleton consists of three main polymers: actin filaments (or microfilaments), microtubules and intermediate filaments, all organized into networks whose architecture is controlled by several classes of regulatory proteins. These three groups of cytoskeletal polymers differ in their mechanical stiffness, the dynamics of their assembly (polymerization), their polarity and their associated molecular motors [38] and so their continuous remodeling leads to changes in the viscoelastic properties of cells.

Having obtained macrophages by the differentiation of HL60 cells using a method described elsewhere [2, 37], we used specific drugs and chemical agents to perturb cytoskeletal structures thereby altering cell states and then measured the viscoelastic properties as readouts of such alterations. The drugs include blebbistatin (Blebb), which inhibits myosin II and cytochalasin D (CytoD), which depolymerizes filamentous actin in the cell. Details of these pharmacological interventions are reported in our previous work [2, 3, 39]. Furthermore, macrophages detect the presence of bacteria using chemical compounds produced by the bacteria, such as N-formylmethionine leucyl-phenylalanine (fMLP). Thus, we tested whether cellular viscoelastic properties are involved in cell function by measuring changes in compliance due to fMLP treatment [2]. All these methods involved specific alterations of the cytoskeleton and the mechanical make-up of the cell. The biomedical significance of these experiments and results engenders the need for further analysis, simulations, curve-fitting and modeling which we now describe in detail in the next section.

2.3. Modeling

2.3.1. “Integer-Order” Mechanical models

Mechanical elements such as linear springs (for elastic response) and linear dashpots (for viscous response) can be combined to form simple models of the viscoelastic properties of materials. Although the models do not convey information about the molecular or microscopic processes going on in the material, they can serve as phenomenological guides giving insight into the nature of the viscoelastic response of materials. Cells respond to constant creep stress in a viscoelastic manner. The input is the stress and the output is the strain. The strain profile can be more or less viscous. Models are very useful for extracting viscoelastic parameters from strain or deformation measurements. We consider six linear mechanical models of creep compliance to choose from, in fitting our experimental data. The equilibrium conditions and constitutive equations for deriving these models are straightforward and details can be found in standard rheology texts [18, 5]. Here, we indicate briefly the mathematical essence of such derivations to aid the acquisition of physical intuition about the resulting equations and models.

First, the Newton model (N), consisting of one dashpot, η_1 has creep compliance given by,

$$J(t) = \frac{1}{\eta_1} t. \quad (2.3)$$

The N model describes the creep compliance of a perfectly viscous body. Eq. 2.3 is obtained by

replacing $\sigma(t)$ in Eq. 1.1b with σ_0 and integrating with respect to time:

$$\sigma_0 = \eta \frac{d\varepsilon}{dt}. \quad (2.4a)$$

$$\sigma_0 \int dt = \eta \int d\varepsilon = \eta\varepsilon + c, \quad (2.4b)$$

where c is a constant of integration to be determined by initial conditions. For the N model, c is 0. Other models are derived from the equilibrium conditions and constitutive relations by similar substitution of the σ_0 and direct integration. Next is the so-called Maxwell model (M), made up of a spring and a dashpot in series, such that the creep compliance can be expressed as

$$J(t) = \frac{1}{E_1} + \frac{1}{\eta_1}t. \quad (2.5)$$

In the M model, the constant of integration (Eq. 2.4b) is not 0 because there is an instantaneous elasticity provided by the Hookean spring. Third is the Kelvin model which is also called the Voigt model. Throughout this work, we denote it as the Kelvin-Voigt model (KV). The KV model has a spring and dashpot in parallel. Its creep compliance is denoted thus:

$$J(t) = \frac{1}{E_2} \left(1 - e^{-\frac{E_2}{\eta_2}t} \right). \quad (2.6)$$

A spring and a KV element combined in series give the so-called Standard Linear Solid (SLS) or Zener model with creep compliance given by

$$J(t) = \frac{1}{E_1} + \frac{1}{E_2} \left(1 - e^{-\frac{E_2}{\eta_2}t} \right). \quad (2.7)$$

When a dashpot is linked in series with a KV element, we get the Standard Linear Liquid model (SLL) whose creep compliance has the form

$$J(t) = \frac{1}{\eta_1}t + \frac{1}{E_2} \left(1 - e^{-\frac{E_2}{\eta_2}t} \right). \quad (2.8)$$

A sixth mechanical model is called the Burgers model (B), consisting of a KV element and a Maxwell model in series. The creep compliance is expressed as

$$J(t) = \frac{1}{E_1} + \frac{1}{\eta_1}t + \frac{1}{E_2} \left(1 - e^{-\frac{E_2}{\eta_2}t} \right). \quad (2.9)$$

The creep part of the strain or deformation (from which the creep compliance is derived by simple normalization) for the Burgers model and all the other five mechanical models are illustrated in Fig. 1. In view of a transition to fractional order models, we state explicitly the constitutive equations for N, M, KV, SLS, SLL and B. For N, the constitutive equation is

$$\sigma(t) = b_1 \frac{d}{dt} \varepsilon(t), \quad (2.10)$$

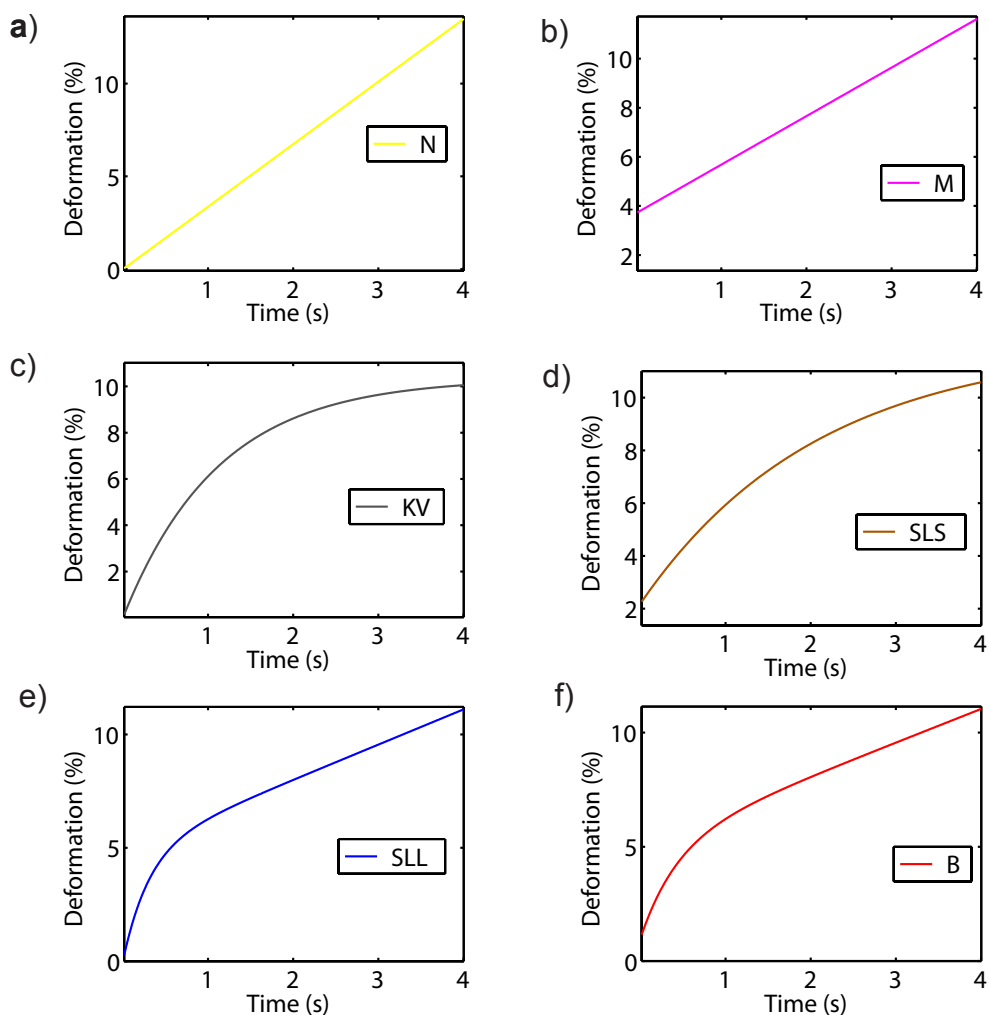


Figure 1. The creep part of the strain or deformation for all six mechanical models. a) Newton model, N. b) Maxwell model, M. c) Kelvin-Voigt model, KV. d) Standard linear solid model, SLS. e) Standard linear liquid, SLL. f) Burgers model, B. The models were plotted using the same input parameter, namely, a strain function of time ranging from 0 to 11% for 4 s, chosen as an example giving strain/compliance shapes typical of the cells we have measured.

where $b_1 = \eta_1$, when this equation is solved for the creep case when $\sigma(t) = \sigma_0$. The constants a_k and b_k are determined for each model accordingly. The constitutive equation for M is

$$\sigma(t) + a_1 \frac{d\sigma}{dt} = b_1 \frac{d}{dt} \varepsilon(t). \quad (2.11)$$

It is

$$\sigma(t) = m\varepsilon(t) + b_1 \frac{d}{dt} \varepsilon(t), \quad (2.12)$$

for the KV model.

For SLS, it is

$$\left(1 + a_1 \frac{d}{dt}\right) \sigma(t) = \left(m + b_1 \frac{d}{dt}\right) \varepsilon(t). \quad (2.13)$$

And for SLL, we have

$$\left(1 + a_1 \frac{d}{dt}\right) \sigma(t) = \left(b_1 \frac{d}{dt} + b_2 \frac{d^2}{dt^2}\right) \varepsilon(t). \quad (2.14)$$

The constitutive equation for the Burgers' 4-element model is

$$\sigma(t) + \left(\frac{\eta_1}{E_1} + \frac{\eta_1}{E_2} + \frac{\eta_2}{E_2}\right) \dot{\sigma}(t) + \frac{\eta_1 \eta_2}{E_1 E_2} \ddot{\sigma}(t) = \eta_1 \dot{\varepsilon}(t) + \frac{\eta_1 \eta_2}{E_2} \ddot{\varepsilon}(t) \quad (2.15)$$

It is straightforward to rename the elastic and viscous constants in order to obtain a compact expression:

$$\left(1 + a_1 \frac{d}{dt} + a_2 \frac{d^2}{dt^2}\right) \sigma(t) = \left(b_1 \frac{d}{dt} + b_2 \frac{d^2}{dt^2}\right) \varepsilon(t), \quad (2.16)$$

where $a_1 = \left(\frac{\eta_1}{E_1} + \frac{\eta_1}{E_2} + \frac{\eta_2}{E_2}\right)$, $a_2 = \frac{\eta_1 \eta_2}{E_1 E_2}$, $b_1 = \eta_1$ and $b_2 = \frac{\eta_1 \eta_2}{E_2}$.

Clearly, Eq.2.16 has the following general form

$$\left(1 + \sum_{k=1}^p a_k \frac{d^k}{dt^k}\right) \sigma(t) = \left(m + \sum_{k=1}^q b_k \frac{d^k}{dt^k}\right) \varepsilon(t), \quad (2.17)$$

where, for the Burgers' model $m = 0$ and $p = q = 2$. At this stage, p and q are integers and to meet physical requirements, $q = p$ or $q = p + 1$, while a_k , b_k and m are non-negative constants. For N, $m = 0$, $p = 0$ and $q = 1$, for M, $m = 0$ and $p = q = 1$, for KV, $m > 0$ and $p = 0$ $q = 1$, for SLS, $m > 0$ and $p = q = 1$ and for SLL, $m = 0$, $p = 1$ and $q = 2$. Thus, we can use Eq. 2.17 to generate all the material constants for the SLL, SLS, KV, M, and N models, and also have it as a synthesis of the various formalisms (integral, differential, matrices and geometric construction) used in obtaining the models. We next use Eq. 2.17 for a transition to fractional calculus-based models of viscoelasticity. Anecdotaly, there are alternatives to mechanical models, other than fractional element models. Power law models are among such alternatives which we also used in [2]. Only the overlapping insights from both power-law and mechanical models impinge upon the conclusions of our work, hence, our work does not address the ongoing debate as to whether cellular viscoelastic behaviors truly follow

power-laws [40, 41] or mechanical models [42, 36]. Rather, we present our finding that fractional calculus modeling of cellular viscoelasticity is a general framework for characterizing cellular behavior, a framework of which both integral order mechanical models and integral order power law models are but parts, as has been reviewed recently [16].

2.3.2. Fractional calculus models

Consider the constitutive equation for the Burgers' 4-element model (Eq.2.17). Without undermining linearity and without any loss of generality, Eq.2.17 can be expressed as

$$\left(1 + \sum_{k=1}^p a_k \frac{d^{\nu_k}}{dt^{\nu_k}}\right) \sigma(t) = \left(m + \sum_{k=1}^q b_k \frac{d^{\nu_k}}{dt^{\nu_k}}\right) \varepsilon(t), \quad (2.18)$$

where $\nu \in 0, 1$ and $\nu_k = k + \nu - 1$. As long as ν is either 0 or 1, then we have integer order derivative in Eq.2.18. Also, Eq.2.18 is the constitutive relation for linear viscoelasticity in differential form. It's integral form usually adopts the so-called Boltzmann superposition principle to present strain as the result of stress. Let us focus on the differential form of the constitutive relation (Eq.2.18). If ν is allowed to be continuous between 0 and 1, then we have fractional order derivatives. This plunges us into the sea of fractional calculus, engendering fractional element modeling of cellular viscoelasticity. More explicitly, within the linear viscoelastic regime, as we showed in the introduction, the mechanical properties of the material can be separated into an elastic recoverable part as Hooke's law (Eq. 1.1a) represented by a spring, and the viscous part as Newton's law (Eq. 1.1b) [5], represented by a dashpot. Fractional order derivatives allow us to combine the spring and the dashpot into the so-called spring-pot [23] thus:

$$\sigma(t) = E \frac{d^0 \varepsilon}{dt^0} \text{ (spring)} \quad (2.19a)$$

$$\sigma(t) = \eta \frac{d^1 \varepsilon}{dt^1} \text{ (dashpot)} \quad (2.19b)$$

$$\sigma(t) = \eta \frac{d^\nu \varepsilon}{dt^\nu} \text{ (springpot)}, \quad (2.19c)$$

where ν is allowed to vary continuously between 0 and 1. Almost prereflexively, we can glimpse fractional order mechanical models as series/parallel combinations of springs and springpots. For historical reasons, springpots are called Scott-Blair elements [43, 6].

Using springpots (Eq. 2.19c) the fractional order constitutive equation for B can be written as a further generalization of 2.18:

$$\left(1 + a_1 \frac{d^\nu}{dt^\nu} + a_2 \frac{d^2}{dt^{1+\nu}}\right) \sigma(t) = \left(b_1 \frac{d^\nu}{dt^\nu} + b_2 \frac{d^{1+\nu}}{dt^{1+\nu}}\right) \varepsilon(t), \quad (2.20)$$

Details of the derivation of the fractional order constitutive equations and compliance for the models we are using (N, M, KV, SLL, SLS and B) can be found in [44, 45, 46]. We have followed closely the notation in [44], in order not to worsen the current situation in the fractional calculus field where diverse notations and formalisms tend to obfuscate the underlying mathematical unity. The fractional order expressions of strain for B, SLL, SLS, KV and M can all be found in [6], where Mainardi in particular has derived them with rigor and elegance. We used these expressions in fitting the compliance data.

2.3.3. Implementation and curvefitting in Matlab

Caputo and Mainardi connected linear viscoelastic models with fractional order models back in the early 1970s [47, 43] and introduced the following very useful correspondence principles which make it less laborious to move from classical viscoelastic models to fractional order models [47, 6]:

$$0 < \nu < 1 \begin{cases} t \rightarrow \frac{1}{\Gamma(1+\nu)} \left(\frac{t}{\tau_0}\right)^\nu \\ \delta(t) \rightarrow \frac{1}{\Gamma(1-\nu)} \left(\frac{t}{\tau_0}\right)^{-\nu} \\ e^{-\frac{t}{\lambda}} \rightarrow E_\nu \left(-\frac{t}{\lambda}\right), \end{cases} \quad (2.21)$$

where λ denotes the relaxation time, E_ν is a generalized exponential function called the Mittag-Leffler function (mlf) (see [44] for details), here, of order ν and $\delta(t)$ is the Dirac delta distribution. Mainardi and Spada [44] have provided transparent expressions for both the mechanical models and their FC versions ready for implementation in programs such as MATLAB. We used their expressions [44] for fractional versions of M, KV, SLS and SLL in the case of creep for fitting cell compliance data. For instance, the FC version of KV (Frac KV) is represented by a Hookean spring and a springpot or Scott-Blair element. The Frac KV constitutive relation is therefore

$$\sigma(t) = E\varepsilon(t) + \eta \frac{d^\nu \varepsilon}{dt^\nu}, \quad (2.22)$$

where for clarity, m and b_1 in Eq 2.12 are the the elastic modulus and coefficient of viscosity, respectively. The creep compliance for the Frac KV, following the notation in [44] and our expression for KV in Eq 2.6, is

$$J(t) = \frac{1}{E_2} \left(1 - E_\nu \left(-\frac{E_2}{\eta_2} t^\nu \right) \right). \quad (2.23)$$

Thus, we are able to make direct comparisons between the parameters from the integer order mechanical models and their FC versions. The MATLAB function for the mlf is publicly available [48]. Using the mlf, we developed an in-house MATLAB routine that implements least-squares curve-fitting for both integer order and fractional order mechanical models.

3. Results and discussion

3.1. Integer order mechanical models fit cell compliance data

Commonly used integer order mechanical models do in fact fit cell compliance data well, including the compliance data of macrophages as we show in Fig. 2. Each of the models produced meaningful parameters (see Table 1) for characterizing the viscoelastic properties of macrophages. As shown in Table 1, in terms of producing physically meaningful parameters as well as the goodness of fit parameters which are relevant here for comparing the models, the SLL is the best of the four mechanical models. Note that the goodness of fit parameters are the sum of squared errors (sse), coefficient of determination (rsquare), adjusted coefficient of determination (adjusted rsquare) and the root-mean-square error (rmse). In all the tables, dfe refers to the degrees of freedom (number of cells fitted).

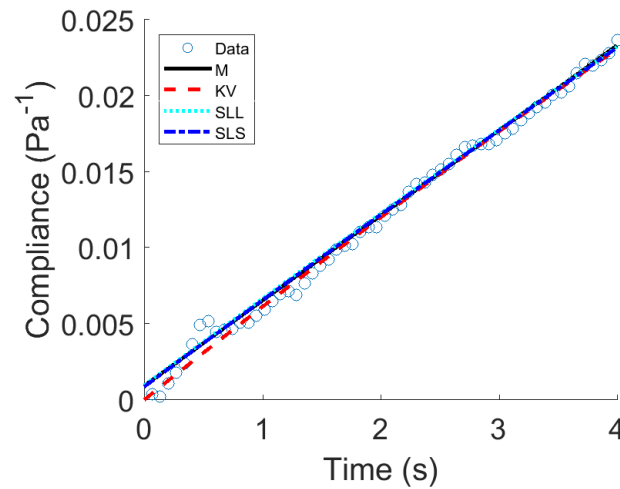


Figure 2. Integer order mechanical models. The average creep compliance of macrophages are fitted using four models, M, KV, SLS and SLL.

Table 1. Parameters of integer order mechanical models

Parameters	M	KV	SLL	SLS
E_1	1081.47	0	0	1166.70
η_1	178.65	0	1038.97	0
E_2	0	6.33	2.64	174.19
η_2	0	160.38	174.38	2.50
sse	1.7645E-05	1.4958E-05	2.0961E-05	1.8046E-05
rsquare	0.9931	0.9942	0.9918	0.9930
dfe	57	57	56	56
adjusted rsquare	0.9930	0.9941	0.9915	0.9927
rmse	0.0006	0.0005	0.0006	0.0006

3.2. Partial failure of integer order mechanical models

However, when the viscoelastic properties of the macrophages were carefully altered using drugs and following their maturation (at 96 hours or h96), none of the integer models fitted all the data while producing meaningful parameters (see Table 2). Each had limitations as shown in Fig. 3. When macrophages were treated with cytochalasin D (CD) which depolymerizes filamentous actin in the cell, the M model clearly failed to include data from the first 0.6 seconds, rendering the fit spurious, even from a cursory visual inspection. For macrophages treated with blebbistatin (Blebb) which inhibits myosin II, SLL is a poor fit. For fMLP-treated cells, KV is a poor fit. For more mature macrophages (96h), SLS is a poor fit. These limitations are further seen in the table of parameters (Table 2) where rmse increases, rsquare and adjusted rsquare decrease reflecting the poor fitting seen in the figure (Fig. 3). Moreover, the results were not stable during repeated fitting routines, as were those of Table 1.

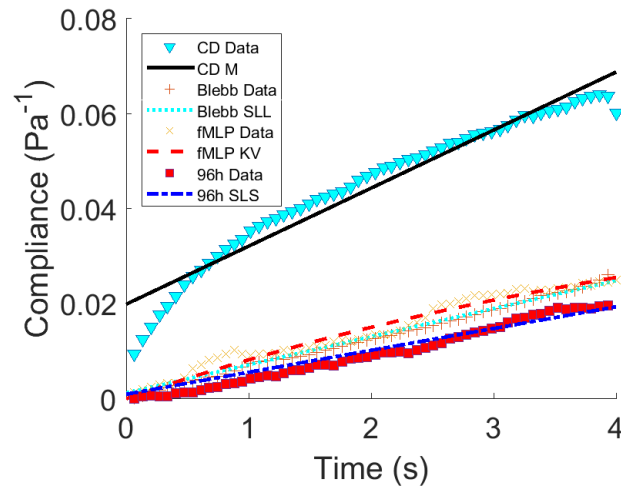


Figure 3. Failures of integer order mechanical models. Instances where the four models, M, KV, SLS and SLL, failed to fit and produce meaningful parameters. M failed when macrophages were treated with CD. For Blebb-treated macrophages, SLL is a poor fit. For fMLP-treated cells, KV is a poor fit. For more mature macrophages (96h), SLS is a poor fit.

Table 2. Parameters for failures of integer order mechanical models

Parameters	CD_M	fMLP_KV	Blebb_SLL	h96_SLS
E_1	50.19	0	0	1027.58
η_1	81.86	0	797.36	0
E_2	0	20.21	0.12	215.15
η_2	0	111.30	168.95	1.08
sse	0.0007	0.0001	2.5368E-05	0.0001
rsquare	0.9473	0.9650	0.9914	0.9516
dfe	57	57	55	55
adjusted rsquare	0.9464	0.9643	0.9911	0.9498
rmse	0.0034	0.0014	0.0007	0.0014

Table 3. Parameters from fractional calculus mechanical models

Parameters	Frac_M	Frac_KV	Frac_SLL	Frac_SLS
E_1	40977.27	0	0	3168.98
η_1	164.23	0	127.95	0
E_2	0	0.91	8184.51	164.67
η_2	0	163.23	591.95	2.28
ν	0.94	0.95	0.66	0.96
sse	1.4117E-05	1.4222E-05	0.0002	1.5576E-05
rsquare	0.9945	0.9944	0.9249	0.9939
dfc	56	56	55	55
adjusted rsquare	0.9942	0.9942	0.9208	0.9936
rmse	0.0005	0.0005	0.0019	0.0005

3.3. FC mechanical models fit cell compliance data

Using the same macrophage compliance data as in Fig. 2, we found that the FC mechanical models fit the data well, as shown in Fig. 4. Based on the table of viscoelastic parameters and the goodness of fits (Table 3), the Frac KV model is the best for this set of macrophage data. It has the best adjusted rsquare, along with M, but unlike M, the viscoelastic parameters are stable of several iterations. The instability in using M is shown in the elastic modulus from M, with five orders of magnitude (40977 Pa).

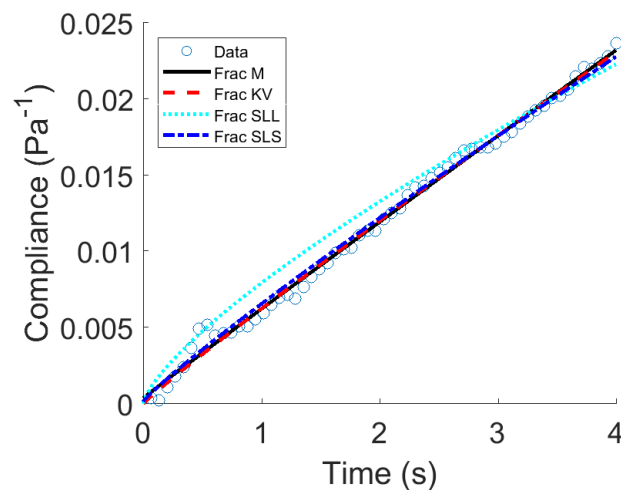


Figure 4. Fractional calculus mechanical models. The average creep compliance of macrophages are fitted using four FC models, Frac M, Frac KV, Frac SLS and Frac SLL.

3.4. FC mechanical models quantify cytoskeletal changes

Having found that Frac KV is the best in fitting compliance data of macrophages, we went further to use this model to fit compliance data for macrophages subjected to pharmacological interventions. Interestingly, we also found that Frac KV fits well and produces meaningful parameters that quantify

Table 4. Frac KV model parameters that quantify drug-induced changes

Parameters	Ctl_Frac_KV	Blebb_Frac_KV	CD_Frac_KV	fMLP_Frac_KV
E_2	0.91	0.17	3.88	0.32
η_2	163.23	155.52	29.47	125.13
ν	0.95	0.98	0.53	0.80
sse	1.4222E-05	8.9647E-06	2.8295E-05	9.0973E-05
rsquare	0.9944	0.9970	0.9977	0.9695
dfe	56	55	56	56
adjusted rsquare	0.9942	0.9968	0.9976	0.9684
rmse	0.0005	0.0004	0.0007	0.0013

drug-induced alterations of cell viscoelastic properties as shown in Fig. 5. The parameters enable

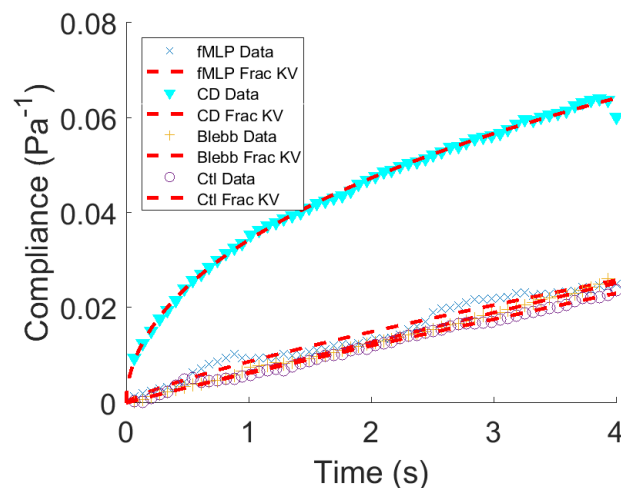


Figure 5. Fractional calculus KV model quantifies drug-induced changes in cell viscoelastic properties. The drugs CD, Blebb and the chemoattractant fMLP have known specific effects on cell cytoskeleton.

viscoelastic characterization of drug responses. In Table 4, the elastic and viscous constants change in drug-dependent fashion since these drugs have generic effects on cells depending on whether they are adherent or in suspension. Our macrophages were measured in suspension [2, 3]. The steady state viscosity, η_2 , decreases from 163 Pa.s to 29 Pa.s following the treatment of macrophages with cytochalasin D, which means a reduction in the cell's resistance to flow. Not surprisingly, the elastic modulus, E_2 , increases by an order of magnitude from 0.91 Pa to 3.88 Pa. With blebbistatin treatment, Frac KV model reveals a decrease in elastic modulus and a decrease in steady state viscosity. These results are in consonance with the already noted peculiar responses of macrophages to blebbistatin, compared to many other adherent but suspended cells [3].

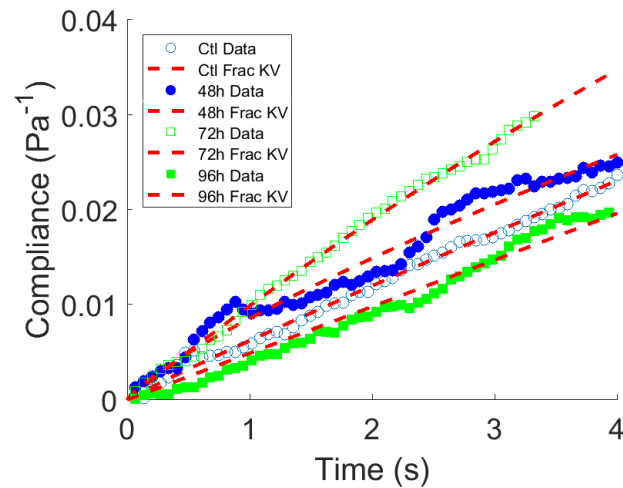


Figure 6. Fractional calculus KV model quantifies changes in cell viscoelastic properties due to cell cycling and maturation. From 24 h following induction of differentiation to 96 h, the macrophages exhibit cell cycling induced changes in their cytoskeleton apparent in the fit parameters

Table 5. Parameters from Frac KV model reflecting cell cycling and maturation

Parameters	Ctl_Frac_KV	h48h_Frac_KV	h72h_Frac_KV	h96h_Frac_KV
E_2	0.91	0.82	8.48	0.0038
η_2	163.23	124.74	96.86	203.77
ν	0.95	0.80	0.99	0.99
sse	1.4222E-05	9.1126E-05	9.7456E-06	5.1307E-05
rsquare	0.9931	0.9694	0.9973	0.97709
dfe	56	56	46	55
adjusted rsquare	0.9942	0.9684	0.9972	0.9763
rmse	0.0005	0.0013	0.0005	0.0010

3.5. FC mechanical models quantify cell cycle changes during maturation

In addition to quantifying viscoelastic changes due to pharmacological interventions, the fractional KV model also quantifies known cytoskeletal changes due to cell cycling and maturation of the cells, as shown in Fig. 6. Both the steady viscosity and the elastic modulus quantify changes as macrophages mature (Table 5). From the induction of differentiation to 72 hours after, there is a gradual reduction in steady state viscosity η_2 . Interestingly, apoptosis (cell death) sets in around 96 hours following differentiation [2, 37]. The steady state viscosity jumps to a value greater than those of healthy cells. Succinctly, we have used fractional calculus models to further characterize inherent biophysical parameters of cells which are already known to be useful diagnostic parameters [21]. In fact, since recent work also present cell and tissue mechanical properties as novel therapeutic targets in the case of cancer metastasis [28], acute lung injury [39], chronic pulmonary obstructive disease [24], the importance of using more robust and accurate models for extracting viscoelastic parameters of cells and tissues is easy to see.

4. Conclusion

In this work, we have recapitulated some limitations of integer-order mechanical models in capturing features of compliance data from macrophages under various clinically relevant conditions. By comparing fits using both integer order models and fractional calculus versions in Mittag-Leffler form, we found that the viscoelastic parameters from fractional Kelvin-Voigt model quantify the pharmacological interventions and maturation of macrophages more robustly than the integer-order models. Fractional calculus modeling therefore provides robust and more generally applicable biophysical characterization of cells in health and disease.

References

1. Trepate X, Deng L, An S, Navajas D, Tschumperlin D, Gerthoffer W, et al. Universal physical responses to stretch in the living cell. *Nature* 2007;447(7144):592–5. URL: <http://www.nature.com/nature/journal/v447/n7144/abs/nature05824.html>. doi:10.1038/nature05824.
2. Ekpenyong AE, Whyte G, Chalut K, Pagliara S, Lautenschläger F, Fiddler C, et al. Viscoelastic Properties of Differentiating Blood Cells Are Fate- and Function-Dependent. *PLoS ONE* 2012;7(9):e45237. URL: <http://dx.plos.org/10.1371/journal.pone.0045237>. doi:10.1371/journal.pone.0045237.
3. Chan CJ, Ekpenyong AE, Golfier S, Li W, Chalut KJ, Otto O, et al. Myosin II Activity Softens Cells in Suspension. *Biophysical journal* 2015;108(8):1856–69. URL: <http://www.sciencedirect.com/science/article/pii/S0006349515002416>. doi:10.1016/j.bpj.2015.03.009.
4. Mason TG. Rheology of Soft Materials Rheology Rheology - Outline Affine and Non-Affine Shear Deformations. *Soft Materials* 2006;:1–16.
5. Lakes RS. *Viscoelastic Materials*. Cambridge: Cambridge University Press; 2009. ISBN 978-0521885683.

6. Mainardi F. *Fractional Calculus and Waves in Linear Viscoelasticity*. 1 ed.; London: Imperial College Press; 2010. ISBN 9781848163294.
7. Dealy JM. Official nomenclature for material functions describing the response of a viscoelastic fluid to various shearing and extensional deformations. *J Rheol* 1995;39(1):253–65.
8. Kasza KE, Rowat AC, Liu J, Angelini TE, Brangwynne CP, Koenderink GH, et al. The cell as a material. *Curr Opin Cell Biol* 2007;19(1):101–7. URL: <http://www.ncbi.nlm.nih.gov/pubmed/17174543>. doi:10.1016/j.ceb.2006.12.002.
9. Janmey PA, Euteneuer U, Traub P, Schliwa M. Viscoelastic properties of vimentin compared with other filamentous biopolymer networks. *J Cell Biol* 1991;113(1):155–60. URL: <http://www.pubmedcentral.nih.gov/articlerender.fcgi?artid=2288924&tool=pmcentrez&rendertype=abstract>.
10. Ingber DE. Tensegrity: the architectural basis of cellular mechanotransduction. *Annu Rev Physiol* 1997;59:575–99. URL: <http://www.ncbi.nlm.nih.gov/pubmed/9074778>. doi:10.1146/annurev.physiol.59.1.575.
11. Stamenović D. Rheological behavior of mammalian cells. *Cell Mol Life Sci* 2008;65(22):3592–605. URL: <http://www.ncbi.nlm.nih.gov/pubmed/18668200>. doi:10.1007/s00018-008-8292-y.
12. Otto O, Rosendahl P, Mietke A, Golfier S, Herold C, Klaue D, et al. Real-time deformability cytometry: on-the-fly cell mechanical phenotyping. *Nature methods* 2015;12(3):199–202. URL: <http://dx.doi.org/10.1038/nmeth.3281>. doi:10.1038/nmeth.3281.
13. Man SM, Ekpenyong A, Tourlomousis P, Achouri S, Cammarota E, Hughes K, et al. Actin polymerization as a key innate immune effector mechanism to control Salmonella infection. *Proceedings of the National Academy of Sciences of the United States of America* 2014;111(49). URL: <http://www.ncbi.nlm.nih.gov/pubmed/25422455>. doi:10.1073/pnas.1419925111.
14. Wu PH, Aroush DRB, Asnacios A, Chen WC, Dokukin ME, Doss BL, et al. A comparison of methods to assess cell mechanical properties. *Nature Methods* 2018;15(7). URL: <https://pubmed.ncbi.nlm.nih.gov/29915189/>. doi:10.1038/s41592-018-0015-1.
15. Mierke CT. Mechanical Cues Affect Migration and Invasion of Cells From Three Different Directions. 2020. doi:10.3389/fcell.2020.583226.
16. Bonfanti A, Kaplan JL, Charras G, Kabla A. Fractional viscoelastic models for power-law materials. *Soft Matter* 2020a;16(26):6002–20. doi:10.1039/d0sm00354a. arXiv:2003.07834.
17. Bonfanti A, Fouchard J, Khalilgharibi N, Charras G, Kabla A. A unified rheological model for cells and cellularised materials. *Royal Society Open Science* 2020b;7(1). URL: <http://dx.doi.org/10.1098/rsos.190920> <https://doi.org/10.6084/m9.figshare.c.4798338>. doi:10.1098/rsos.190920.
18. Findley WN, Lai JS, Onaran K. *Creep and Relaxation of Nonlinear Viscoelastic Materials*. Dover, 198 ed.; North-Holland; 1976.
19. Lakes RS. Viscoelastic measurement techniques. *Rev Sci Instrum* 2004;75(4):797. doi:10.1063/1.1651639.

20. Guck J, Ananthkrishnan R, Mahmood H, Moon TJ, Cunningham CC, Käs J. The optical stretcher: a novel laser tool to micromanipulate cells. *Biophys J* 2001;81(2):767–84. URL: <http://www.pubmedcentral.nih.gov/articlerender.fcgi?artid=1301552&tool=pmcentrez&rendertype=abstract>. doi:10.1016/S0006-3495(01)75740-2.
21. Guck J, Schinkinger S, Lincoln B, Wottawah F, Ebert S, Romeyke M, et al. Optical deformability as an inherent cell marker for testing malignant transformation and metastatic competence. *Biophys J* 2005;88(5):3689–98. doi:10.1529/biophysj.104.045476.
22. Wottawah F, Schinkinger S, Lincoln B, Ananthkrishnan R, Romeyke M, Guck J, et al. Optical rheology of biological cells. *Phys Rev Lett* 2005a;94(9):1–4. doi:10.1103/PhysRevLett.94.098103.
23. Meral FC, Royston TJ, Magin R. Fractional calculus in viscoelasticity: An experimental study. *Communications in Nonlinear Science and Numerical Simulation* 2010;15(4):939–45. URL: <http://linkinghub.elsevier.com/retrieve/pii/S1007570409002706><http://dx.doi.org/10.1016/j.cnsns.2009.05.004>. doi:10.1016/j.cnsns.2009.05.004.
24. Ionescu C, Lopes A, Copot D, Machado J, Bates J. The role of fractional calculus in modeling biological phenomena: A review. *Communications in Nonlinear Science and Numerical Simulation* 2017;51:141–59. URL: <http://www.sciencedirect.com/science/article/pii/S1007570417301119>. doi:10.1016/j.cnsns.2017.04.001.
25. Lautenschläger F, Paschke S, Schinkinger S, Bruel A, Beil M, Guck J. The regulatory role of cell mechanics for migration of differentiating myeloid cells. *Proc Natl Acad Sci USA* 2009;106(37):15696–701. URL: <http://www.pubmedcentral.nih.gov/articlerender.fcgi?artid=2747182&tool=pmcentrez&rendertype=abstract>. doi:10.1073/pnas.0811261106.
26. Gossett DR, Tse HTK, Lee SA, Ying Y, Lindgren AG, Yang OO, et al. Hydrodynamic stretching of single cells for large population mechanical phenotyping. *Proc Natl Acad Sci USA* 2012;109(20):7630–5. URL: <http://www.pnas.org/cgi/doi/10.1073/pnas.1200107109>. doi:10.1073/pnas.1200107109.
27. Guck J, Chilvers ER. Mechanics meets medicine. *Science translational medicine* 2013;5(212):212fs41. URL: <http://stm.sciencemag.org/content/5/212/212fs41.full>. doi:10.1126/scitranslmed.3007731.
28. Prathivadhi-Bhayankaram SV, Ning J, Mimplitz M, Taylor C, Gross E, Nichols M, et al. Chemotherapy impedes in vitro microcirculation and promotes migration of leukemic cells with impact on metastasis. *Biochemical and Biophysical Research Communications* 2016;479(4):841–6. URL: <http://www.ncbi.nlm.nih.gov/pubmed/27687547><http://linkinghub.elsevier.com/retrieve/pii/S0006291X16315959>. doi:10.1016/j.bbrc.2016.09.121.
29. Van Vliet K, Bao G, Suresh S. The biomechanics toolbox: experimental approaches for living cells and biomolecules. *Acta Mater* 2003;51(19):5881–905. URL: <http://linkinghub.elsevier.com/retrieve/pii/S1359645403005172>. doi:10.1016/j.actamat.2003.09.001.
30. Guck J, Lautenschläger F, Paschke S, Beil M. Critical review: cellular mechanobiology and amoeboid migration. *Integr Biol (Camb)* 2010;2(11-12):575–83. URL: <http://www.ncbi.nlm.nih.gov/pubmed/20871906>. doi:10.1039/c0ib00050g.

31. Di Carlo D. A mechanical biomarker of cell state in medicine. *J Lab Autom* 2012;17(1):32–42. URL: <http://www.ncbi.nlm.nih.gov/pubmed/22357606>. doi:10.1177/2211068211431630.
32. Boyde L, Chalut KJ, Guck J. Interaction of Gaussian beam with near-spherical particle: an analytic-numerical approach for assessing scattering and stresses. *J Opt Soc Am A Opt Image Sci Vis* 2009;26(8):1814–26.
33. Boyde L, Ekpenyong A, Whyte G, Guck J. Comparison of Stresses on Homogeneous Spheroids in the Optical Stretcher Computed with Geometrical Optics and Generalised Lorenz-Mie Theory. *Appl Opt* 2012;:1–25.
34. Chalut KJ, Ekpenyong A, Clegg WL, Melhuish IC, Guck J. Quantifying cellular differentiation by physical phenotype using digital holographic microscopy. *Integr Biol (Camb)* 2012;4(3):280–4. URL: <http://www.ncbi.nlm.nih.gov/pubmed/22262315>. doi:10.1039/c2ib00129b.
35. Ekpenyong AE, Man SM, Achouri S, Bryant CE, Guck J, Chalut KJ. Bacterial infection of macrophages induces decrease in refractive index. *Journal of biophotonics* 2013;6(5):393–7. URL: <http://www.ncbi.nlm.nih.gov/pubmed/22887897>. doi:10.1002/jbio.201200113.
36. Wottawah F, Schinkinger S, Lincoln B, Ebert S, Müller K, Sauer F, et al. Characterizing single suspended cells by optorheology. *Acta Biomater* 2005b;1:263–71.
37. Ekpenyong AE. Viscoelastic and optical properties of blood stem cells : from differentiation to activation and infection. Ph.D. thesis; University of Cambridge, PhD Thesis; 2012. URL: https://books.google.com/books/about/Viscoelastic_{_}and_{_}Optical_{_}Properties_{_}of_{_}B.html?id=t5nVoQEACAAJhttp://ethos.bl.uk/OrderDetails.do?uin=uk.bl.ethos.610649.
38. Fletcher DA, Mullins RD. Cell mechanics and the cytoskeleton. *Nature* 2010;463(7280):485–92. doi:10.1038/nature08908.
39. Ekpenyong A, Toepfner N, Fiddler C, Herbig M, Li W, Cojoc G, et al. Mechanical deformation induces depolarization of neutrophils. *Science Advances* 2017;3(6). doi:10.1126/sciadv.1602536.
40. Kollmannsberger P, Fabry B. Linear and Nonlinear Rheology of Living Cells. *Annu Rev Mater Res* 2010;41(1):110301100446097. URL: <http://www.annualreviews.org/doi/abs/10.1146/annurev-matsci-062910-100351>. doi:10.1146/annurev-matsci-062910-100351.
41. Lenormand G, Millet E, Fabry B, Butler JP, Fredberg JJ. Linearity and time-scale invariance of the creep function in living cells. *J R Soc Interface* 2004;1(1):91–7. URL: <http://www.pubmedcentral.nih.gov/articlerender.fcgi?artid=16189333&tool=pmcentrez&rendertype=abstract>. doi:10.1098/rsif.2004.0010.
42. Karcher H, Lammerding J, Huang H, Lee RT, Kamm RD, Kaazempur-Mofrad MR. A three-dimensional viscoelastic model for cell deformation with experimental verification. *Biophys J* 2003;85(5):3336–49. URL: <http://www.pubmedcentral.nih.gov/articlerender.fcgi?artid=1303611&tool=pmcentrez&rendertype=abstract>. doi:10.1016/S0006-3495(03)74753-5.
43. Loverro A. Fractional Calculus: History, Definitions and Applications for the Engineer. Tech. Rep.; Department of. Aerospace and Mechanical Engineering, University of Notre Dame; 2004.

44. Mainardi F, Spada G. Creep, relaxation and viscosity properties for basic fractional models in rheology. *Eur Phys J* 2011;193(1):133–60. URL: <http://www.springerlink.com/index/10.1140/epjst/e2011-01387-1>. doi:10.1140/epjst/e2011-01387-1.
45. Dalir M, Bashour M. Applications of Fractional Calculus. *Math Probl Eng* 2010;4(21):1021–32.
46. Zhou H, Wang C, Han B, Duan Z. A creep constitutive model for salt rock based on fractional derivatives. *Int J Rock Mech Min Sci* 2011;48(1):116–21. URL: <http://linkinghub.elsevier.com/retrieve/pii/S1365160910002066>. doi:10.1016/j.ijrmms.2010.11.004.
47. Caputo M, Mainardi F. Linear models of dissipation in anelastic solids. *Riv Nuovo Cimento* 1971;1(2):161–98.
48. Podlubny I. Mittag-Leffler function. 2012. URL: <https://www.mathworks.com/matlabcentral/fileexchange/8738-mittag-leffler-function>.

Acknowledgments

The authors are grateful to Prof Dr Jochen Guck of Max Planck Institute for the Science of Light, in whose Laboratory in the University of Cambridge, A. Ekpenyong, carried out all the compliance measurements modeled in this work. Funding: This work was supported by Creighton University's College of Arts and Sciences startup grant to A. Ekpenyong (240133-215000 FY19) and by a Creighton University Ferlic Scholarship to A. Vo.

Conflict of interest

The authors declare there is no conflict of interest.



AIMS Press

©2021 the Author(s), licensee AIMS Press. This is an open access article distributed under the terms of the Creative Commons Attribution License (<http://creativecommons.org/licenses/by/4.0>)